Journal of Solid State Chemistry 276 (2019) 152–158

Contents lists available at ScienceDirect

Journal of Solid State Chemistry

journal homepage: www.elsevier.com/locate/jssc

Heat capacity, thermal expansion and sensitivity to hydrostatic pressure of $(NH_4)_3SiF_7$ at successive structural phase transitions

Evgeniy V. Bogdanov [a,b,*], Evgeniy I. Pogoreltsev [a,c], Mikhail V. Gorev [a,c], Andrey V. Kartashev [a,d], Natalia M. Laptash [e], Igor N. Flerov [a,c]

[a] Kirensky Institute of Physics, Federal Research Center KSC SB RAS, Krasnoyarsk, Russia
[b] Institute of Engineering Systems and Energy, Krasnoyarsk State Agrarian University, 660049 Krasnoyarsk, Russia
[c] Institute of Engineering Physics and Radioelectronics, Siberian Federal University, Krasnoyarsk, Russia
[d] Astafijev Krasnoyarsk State Pedagogical University, 660049 Krasnoyarsk, Russia
[e] Institute of Chemistry, Far Eastern Department of RAS, 690022 Vladivostok, Russia

ARTICLE INFO

Keywords:
Phase transition
Fluorides
Heat capacity
Entropy
Thermal expansion
High pressure

ABSTRACT

Heat capacity, thermal dilatation, permittivity and sensitivity to external pressure of $(NH_4)_3SiF_7$ were studied. Due to the absence of cubic phases $Pm\bar{3}m$ and $Pa\bar{3}$, a strong decrease in the total entropy change $\sum \Delta S_i = 19$ J/mol K associated with four successive transformations $P4/mbm \leftrightarrow Pbam \leftrightarrow P2_1/c11 \leftrightarrow P\bar{1} \leftrightarrow P12_1/c1$ was found in silicate in comparison with other double fluoride salts $(NH_4)_3MeF_7$ (Me: Ge, Ti, Sn) Using analysis of the excess heat capacity in the framework of the thermodynamic theory, the entropies associated with each individual phase transition were determined. In accordance with the entropic parameters, the complete ordering of the structural elements occurs in the monoclinic phase $P2_1/c11$. Further change in symmetry is associated with small entropy changes which prove insignificant displacement of structural units. A $T-p$ phase diagram was constructed and good agreement was found between measured and calculated baric coefficients.

1. Introduction

As usual, crystal structure of the complex fluoride compounds is very sensitive to a change of the chemical pressure and the external parameters such as temperature and hydrostatic pressure and demonstrates a rich variety of the symmetry [1–7]. In this respect, a series of the double fluoride salts $(NH_4)_3MeF_7 = (NH_4)_2MeF_6 \cdot NH_4F = (NH_4)_3[MeF_6]F$ (Me: Si, Ge, Ti, Sn) is a good example because they were found to undergo a variety of the unique or successive structural phase transitions sometimes associated with the reconstructive processes leading to increase of the symmetry under cooling which is very rare [8–15].

Large changes in entropy and elastic strain associated with many transformations indicate the main contribution of the ordering of some structural units which prove the models of structural distortions suggested on the results of X-ray diffraction observations. On the other hand, both of these values are very important parameters to realize significant barocaloric effect which allows to consider $(NH_4)_3MeF_7$ compounds as promising materials to design effective solid state refrigerants [16,17]. In accordance with the group-theoretical analysis, the parent phase of double fluoride salts was postulated as a cubic one (sp. gr. $Pm\bar{3}m$) [8]. However, at atmospheric pressure, this cubic phase was experimentally observed only in compounds with large Me atoms: $(NH_4)_3PbF_7$ [18] and $(NH_4)_3SnF_7$ at room and high temperature, respectively [11,12]. At high pressure, $Pm\bar{3}m$ phase was suggested in $(NH_4)_3TiF_7$ undergoing succession of transformations $Pm\bar{3}m \leftrightarrow 4/m \leftrightarrow P4/mnc \leftrightarrow Pa\bar{3}$ [10]. Further decrease in the size of the central atom led to the absence of $Pm\bar{3}m$ phase in $(NH_4)_3GeF_7$ $(P4/mbm(G1) \leftrightarrow Pbam(G2) \leftrightarrow P2_1/c11(G3) \leftrightarrow Pa\bar{3}(G4))$ (Fig. 1) up to the temperature of decomposition even at high pressure [13,14]. However, one can see above that the lowest-temperature phase in germanium compound remains a cubic $Pa\bar{3}$ similar to stannate and titanate which is not connected by the group-subgroup relation with high temperature phases.

The double fluoride salt $(NH_4)_3SiF_7$ characterized by the smallest size of the central atom compared to other $(NH_4)_3MeF_7$ compounds was also known for a long time [18]. However, the pioneering investigation of some its physical properties was performed only recently [15]. Optical and structural studies have allowed to establish some specific features in the behavior of $(NH_4)_3SiF_7$ under temperature variation. First, silicon

* Corresponding author. Kirensky Institute of Physics, Federal Research Center KSC SB RAS, Krasnoyarsk, Russia.
E-mail address: evbogdanov@iph.krasn.ru (E.V. Bogdanov).

https://doi.org/10.1016/j.jssc.2019.04.029
Received 16 January 2019; Received in revised form 28 March 2019; Accepted 22 April 2019
Available online 29 April 2019

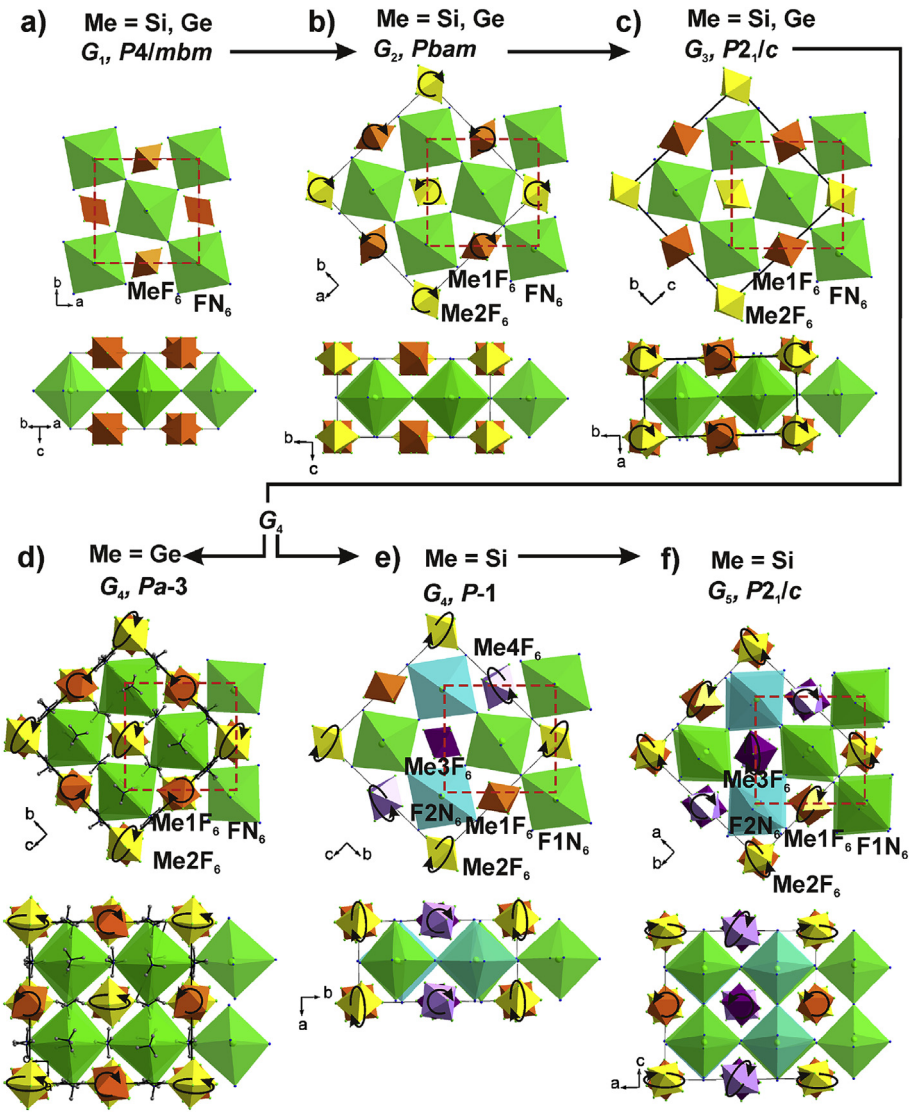

Fig. 1. The main distortions of the $(NH_4)_3MeF_7$ (Me = Si, Ge) crystal structures at phase transitions, leading to rotation of MeF_6 octahedra during the transformations in different projections. Dashed red rectangle surrounds the formula unit of different phases. The sequence of $G_1 \leftrightarrow G_2 \leftrightarrow G_3$ of the phases is the same for both $(NH_4)_3SiF_7$ and $(NH_4)_3GeF_7$, but their $G_3 \leftrightarrow G_4$ phase transitions are different. Further $G_4 \leftrightarrow G_5$ transition exists only in $(NH_4)_3SiF_7$. (For interpretation of the references to colour in this figure legend, the reader is referred to the web version of this article.)

compound undergoes the richest succession of the structural transformations

$(P4/mbm(G1) \leftrightarrow Pbam(G2) \leftrightarrow P2_1/c11(G3) \leftrightarrow P\bar{1}(G4) \leftrightarrow P12_1/c1(G5)$

(Fig. 1) which can be described in the framework of group theoretical approach [15]. Second, the first two phase transitions are identical to those found in germanium double salt. Third, both cubic phases $Pm\bar{3}m$ and $Pa\bar{3}$ found in compounds with Ti and Sn central atoms were not observed. Fourth, $P\bar{1} \leftrightarrow P12_1/c1$ phase transition is accompanied with the appearance of properties characteristic to "proper" ferroelastic. Fifth, the mechanism of all phase transitions was suggested to be associated with the occurrence of N—H···F hydrogen bonds.

This paper focuses on the investigations of the thermodynamic properties at the phase transitions in $(NH_4)_3SiF_7$. Information on the behavior of the heat capacity, entropy, thermal dilatation, permittivity and sensitivity to hydrostatic pressure was obtained and used to discuss the origin and mechanism of structural distortions appeared as a result of the phase transitions.

2. Experimental results

Colorless prismatic single crystals of $(NH_4)_3SiF_7$ were grown by slow evaporation of the aqueous fluoride solution under ambient conditions as it was done in Ref. [15].

The samples for measuring the heat capacity, thermal expansion and permittivity were prepared as quasi-ceramic disk-shaped pellets of 4 mm diameter and 1.0–2.0 mm thickness under pressure without heat treatments because of the presence of ammonium ions. Experiments with differential thermal analysis (DTA) under high pressure were performed on powdered samples of $(NH_4)_3SiF_7$.

The compound synthesized was examined by X-ray diffraction (XRD). The powder diffraction data of $(NH_4)_3SiF_7$ for Rietveld analysis were collected with a Bruker D8 ADVANCE powder diffractometer (Cu-Kα radiation) and linear VANTEC detector. The beam was controlled by the 0.6 mm fixed divergence slit, 6 mm receiving VANTEC slit and Soller slits. The compound $(NH_4)_3SiF_7$ was found to be of a high purity and all lines were indexed by the $P4/mbm$ phase at room temperature (Fig. 2). Cell parameters after refinement (Table 1) were close to those from Ref. [15].

Measurements of thermal expansion were performed using a push-rod dilatometer (NETZSCH model DIL-402C) with a fused silica sample holder. Experiments were carried out in the temperature range 100–300 K with a heating rate of 3 K/min in a dry He flux. In order to remove the influence of system thermal expansion, the results were calibrated by taking quartz as the standard reference. The reproducibility of the data obtained in successive series of the measurements was not less than 5%.

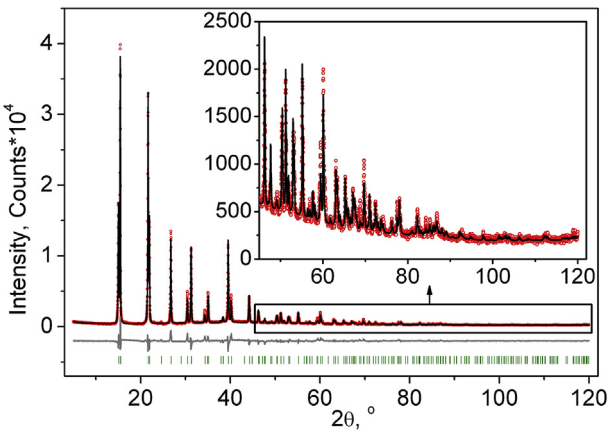

Fig. 2. Difference Rietveld plot of $(NH_4)_3SiF_7$.

Table 1
Main parameters of processing and refinement of the $(NH_4)_3SiF_7$ sample.

Space Group	*P4/mbm*
a, Å	8.0750(2)
b, Å	8.0750(2)
c, Å	5.8613(2)
β, °	90
V, Å^3	382.19(2)
Z	2
R_{wp}, %	10.20
R_p, %	7.72
R_{exp}, %	3.83
χ^2	2.66
R_B, %	4.74

Fig. 3 shows the results of the thermal dilatation measurements on $(NH_4)_3SiF_7$. One can see that in the temperature region of successive phase transitions, the temperature behavior of the volume deformation, $\Delta V/V_0 = 3(\Delta L/L_0)$, and the coefficient of thermal volume expansion, β, is anomalous at all transition points.

The features of the temperature dependence of $\Delta V/V_0(T)$ are as follows: a slight kink at T_1, two small step-wise anomalies at T_2 and T_3 and a very large jump $\delta(\Delta V/V_0) \approx -0.4 \cdot 10^{-2}$ at T_4 (Fig. 3a). The $\beta(T)$ dependence above T_1 was chosen as the lattice contribution β_{Lat} and extrapolated into low temperature phases (Fig. 3b and c). The anomalous contribution, $\Delta\beta = \beta - \beta_{Lat}$, in the thermal dilatation coefficient is positive at $P4/mbm \leftrightarrow Pbam$ and negative at $Pbam \leftrightarrow P2_1/c11 \leftrightarrow P\bar{1} \leftrightarrow P12_1/c1$ phase transitions. The magnitudes of $\Delta\beta_i$ associated with structural transformations are presented in Table 2.

In $(NH_4)_3SiF_7$, the "proper" ferroelastic nature was established only for a low-temperature phase transition at T_4 [15]. To verify that the phase transitions $P4mbm \leftrightarrow Pbam \leftrightarrow P2_1/c \leftrightarrow P\bar{1}$ are not accompanied by the appearance of ferroelectricity, the behavior of the dielectric properties was also studied.

Permittivity and dielectric losses were measured by means of an E7-20 immittance meter at a frequency of 1 kHz upon heating at a rate of about 0.7 K/min in the temperature range 100–300 K. Electrodes on quasi-ceramic pellets were formed by conducting glue covered the opposite flat sides of the sample.

The results of dielectric measurements on $(NH_4)_3SiF_7$ are presented in Fig. 4. We did not find any evidences of the presence of ferroelectricity. The most pronounced anomalies of permittivity and dielectric losses are associated with the phase transitions at T_2 and T_3. Step-wise behavior of both properties ($\Delta\varepsilon_2 \approx \Delta\varepsilon_3 \approx 0.9$; $\Delta tg\delta_2 \approx \Delta tg\delta_3 \approx 2 \cdot 10^{-4}$) confirm the non-ferroelectric origin of the $Pbam \leftrightarrow P2_1/c11$ and $P2_1/c11 \leftrightarrow P\bar{1}$ transformations. Similar behavior of dielectric properties is also characteristic for the ferroelastic phase transition at T_4 ($\Delta\varepsilon_4 \approx 0.3$).

At the high-temperature transformation $P4/mbm \leftrightarrow Pbam$, the $\varepsilon(T)$ anomaly is the smallest while dielectric losses show a pronounced anomalous behavior. A strong gradual increase in $\varepsilon(T)$ and $tg\delta(T)$ above 250 K is associated with the dielectric losses in the quasi-ceramic sample prepared without heat treatment. The results obtained are in good agreement with the data on the temperature behavior of optical and structural properties [15]. All of these experimental facts can be considered as confirmation of the ferroelastic origin of phase transitions in $(NH_4)_3SiF_7$ and the presence of a center of symmetry in all distorted phases.

The effect of hydrostatic pressure on the temperatures of the heat capacity anomalies associated with the phase transitions was experimentally studied by DTA. A powdered sample with a mass of ~0.02 g was placed in a small copper container glued onto one of two junctions of a germanium-copper thermocouple. A quartz sample cemented to the other junction was used as a reference substance.

The system, mounted in such a manner, was placed inside the piston-cylinder type vessel associated with the pressure multiplier. Pressure up to 0.5 GPa was generated using silicon oil as the pressure-transmitting medium. Pressure and temperature were measured with a manganin gauge and copper-constantan thermocouple with accuracies of about ± 10^{-3} GPa and ±0.3 K, respectively. The $T - p$ phase diagram was built using the results of measurements in the process of increasing pressure and temperature (Fig. 5).

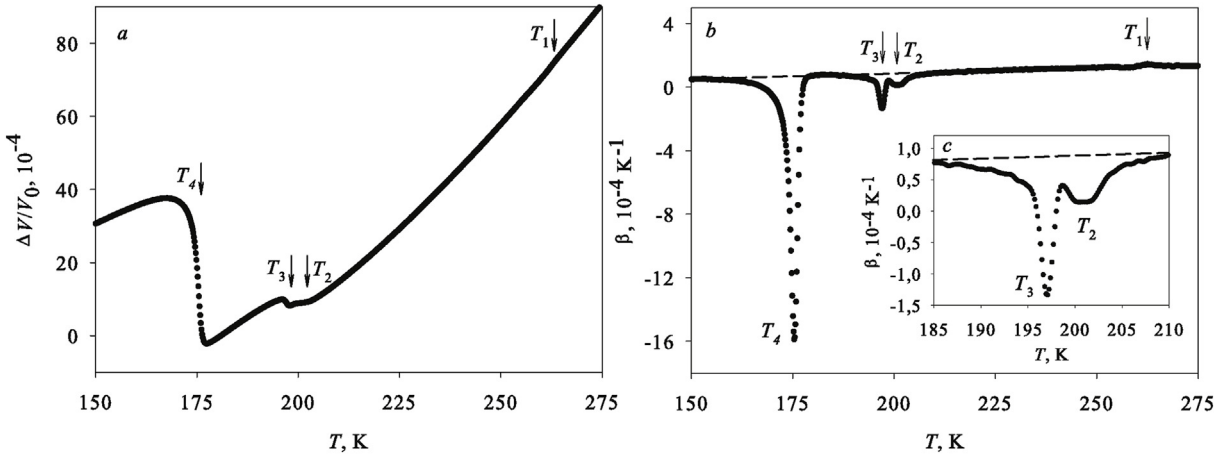

Fig. 3. Temperature dependence of (a) strain $\Delta V/V_0$ and (b) the volume thermal expansion coefficient β of $(NH_4)_3SiF_7$. (c) Anomalous behavior of β at T_2 and T_3. Dashed line is a lattice contribution β_{Lat}.

Table 2
Thermodynamic parameters of the phase transitions in $(NH_4)_3SiF_7$ and $(NH_4)_3GeF_7$ [14]. T_i, K; ΔS_i, J/mol K; dT_i/dp, K/GPa; $\Delta\beta$, 10^{-4} K^{-1}.

Parameters	$(NH_4)_3SiF_7$				$(NH_4)_3GeF_7$		
	G1 - G2	G2 - G3	G3 - G4	G4 - G5	G1 - G2	G2 - G3	G3 - G4
T_i	262.0	199.7	196.5	174.6	277.4	267.8	229.1
ΔS	9.0±1.0	5.3±0.6	1.0±0.2	3.2±0.3	7.5±0.5	4.5±0.3	13.5±1.0
dT_i/dp		−56	−61	−69	10	−47	−34
$\Delta\beta$	0.03	0.80	1.30	17.0	0.3	1.7	33
N	0.18	0.12	0.05		0.11	0.08	

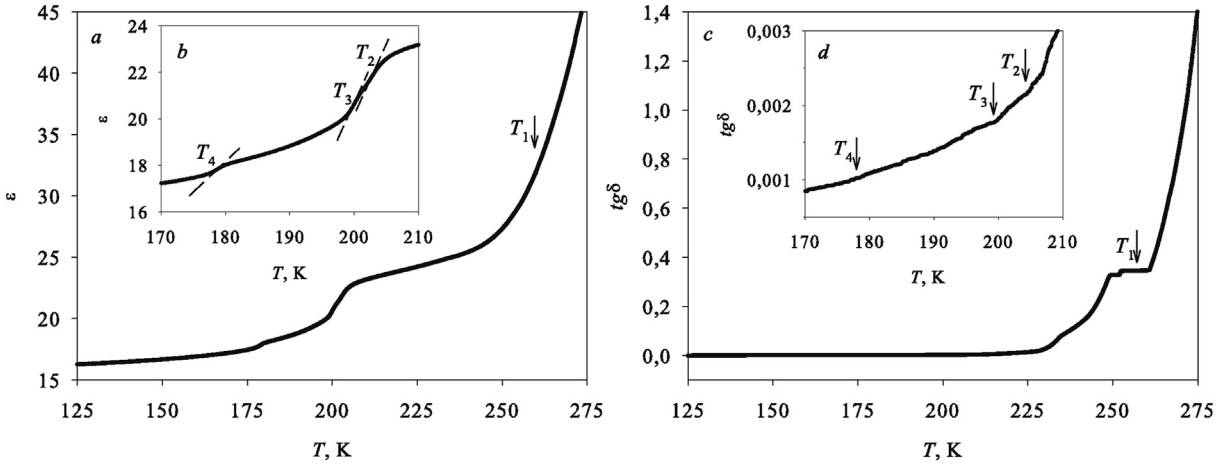

Fig. 4. Temperature dependencies of (a,b) the permittivity ε and (c,d) the dielectric loss tangent $tg\delta$ over a wide temperature range.

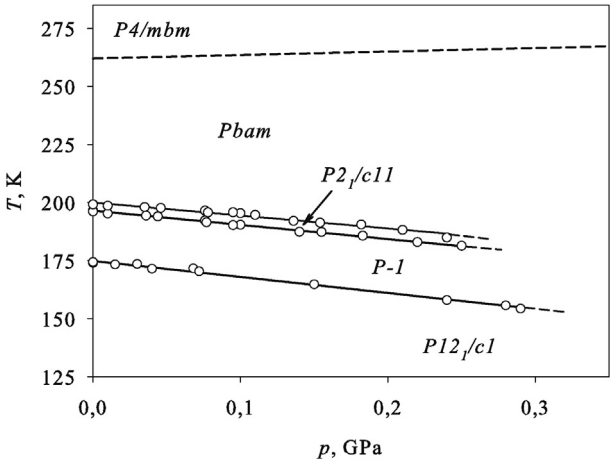

Fig. 5. The temperature-pressure phase diagram of a crystal of $(NH_4)_3SiF_7$. Dashed line shows shift of T_1 under pressure calculated using the Ehrenfest equation.

At atmospheric pressure, four DTA-anomalies associated with a succession of phase transitions in $(NH_4)_3SiF_7$ were observed. However, in accordance with the $T-p$ phase diagram (Fig. 5), only three phase boundaries associated with the following symmetry changes $Pbam \leftrightarrow P2_1/c11 \leftrightarrow P\bar{1} \leftrightarrow P12_1/c1$ were reliably detected with increase in pressure. DTA-anomaly at T_1 was strongly smeared and disappeared at very low pressure. Other three phase transformations are characterized by the negative baric coefficients (Table 2).

The slopes of the phase boundaries for the phase transitions $Pbam \leftrightarrow P2_1/c11$, $P2_1/c11 \leftrightarrow P\bar{1}$ and $P\bar{1} \leftrightarrow P12_1/c1$ are characterized by rather close values (Table 2). It means that the temperature ranges of the $P2_1/c11$ and $P\bar{1}$ phases existence practically do not change with increasing pressure, but they shift towards low temperatures.

A homemade adiabatic calorimeter with three screens [19] was used in order to perform measurements of the heat capacity in a wide temperature range of 82–330 K. The mass of the sample was about 0.3 g. The heat capacity of the "sample + heater + contact grease" system was measured using continuous as well as discrete heating. In the former case, the system was heated at rates of $dT/dt \approx 0.15 - 0.30$ K/min. In the latter case, the calorimetric step was varied from 1.5 to 3.0 K. The inaccuracy in the heat capacity determination did not exceed 0.5%. The heat capacities of the heater and contact grease were determined in individual experiments.

The data obtained by adiabatic calorimeter using stepwise and continuous temperature changes are shown in Fig. 6a. Four anomalies of the molar heat capacity, $C_p(T)$, were found at the temperatures presented in Table 2. Large jump of volume deformation at T_4 observed in thermal expansion measurements on $(NH_4)_3SiF_7$ (Fig. 3) allows one to consider phase transition $P\bar{1} \leftrightarrow P12_1/c1$ as a transformation of the strong first order. That is why temperature regions close to T_4 were also investigated by the method of quasistatic thermograms on heating with small rate of temperature variation $dT/dt \approx 2.5 \cdot 10^{-2}$ K/min. The results of these calorimetric measurements are presented in Fig. 6b. The time dependence of temperature demonstrates that the rather large latent heat $\delta H_4 \approx 500 \pm 50$ J/mol is smeared within the narrow temperature interval $T_4 \pm 0.5$ K that confirms the high quality of the crystal under study. The behavior of thermodynamic properties at T_1, T_2 and T_3 is characteristic for the second order transformations.

3. Discussion

Analysis of thermodynamic data obtained above for silicate, it makes sense to carry out in comparison with the data for the related germanate [14] because the symmetry changes due to phase transitions have in both compounds common and specific features [13,15]. Thermodynamic properties are directly connected with the character of structural distortions and entropy is one of the main thermal parameters giving important additional information to reveal the mechanism of the phase

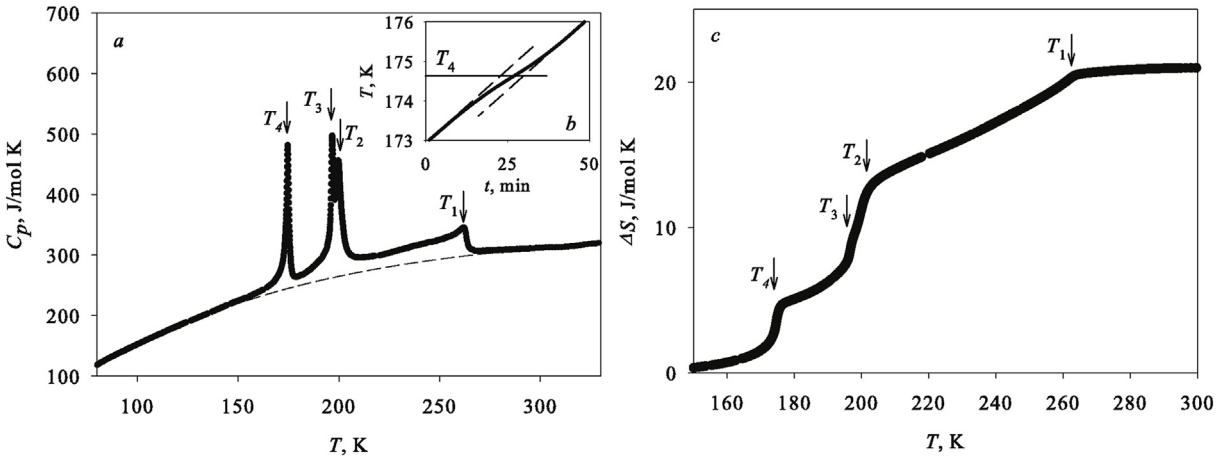

Fig. 6. (a) Temperature dependence of the molar heat capacity in a wide temperature range. Dashed line shows lattice heat capacity. (b) Thermogram in the heating mode in the vicinity of T_4. (c) Temperature dependence of the total excess entropy change.

transitions: order-disorder and displacive.

In order to get information on integral thermodynamic parameters of the phase transitions in $(NH_4)_3SiF_7$, separation of the lattice part, C_{Lat}, and anomalous part, ΔC_p, of the heat capacity has been performed by fitting the experimental data $C_p(T)$ outside the transitions region. For this purpose, a linear combination of Debye's and Einstein's functions, $C_{Lat} = K_D C_D + K_E C_E$, was used. Here

$$C_D(T) = 9R\left(\frac{T}{\Theta_D}\right)^3 \int_0^{\Theta_D/T} \frac{x^4 \exp(x)}{(\exp(x)-1)^2} dx, \quad (1)$$

$$C_E(T) = 3R\left(\frac{\Theta_E}{T}\right)^2 \frac{\exp(\Theta_E/T)}{(\exp(\Theta_E/T)-1)^2} \quad (2)$$

and K_D, K_E, Θ_D and Θ_E are fitting parameters.

Variation of temperature ranges included in the analysis showed that the best performance is obtained when the interval 140 K–280 K is excluded from consideration. In this case, the average deviation of the experimental data from the smoothed curve does not exceed ~0.5%. The lattice contribution is shown as a dashed line in Fig. 6a. One can see that the anomalous heat capacity exists in a wide temperature range and contributions associated with the individual phase transitions are overlapped. That is why it was possible to determine only the values of the total changes of enthalpy, $\sum \Delta H_i = \int \Delta C_p dT = 3900 \pm 300$ J/mol, and entropy, $\sum \Delta S_i = \int (\Delta C_p/T) dT = 19 \pm 1.5$ J/mol K, associated with a sequence of four phase transitions in $(NH_4)_3SiF_7$. The value $\sum \Delta S_i$ is significantly less compared to the same found for related fluorides $(NH_4)_3MeF_7$ (J/mol K): 32 (Me = Ti), 32.5 (Sn), 25.5 (Ge) [10,12,14]. Obviously, this difference is mainly due to the different sequences of the low temperature phase transitions and final structural distortions in these double fluoride salts. In any case, entropy change in silicate, $\sum \Delta S_i = 2.3R \approx R \ln 10$, shows that phase transitions are connected with some ordering/disordering of structural units.

Successive decrease in the symmetry upon cooling from the room temperature, $P4/mbm \leftrightarrow Pbam \leftrightarrow P2_1/c11$, is common peculiarity of both compounds. However, the unit cell volume in initial tetragonal phase in silicate is less than in germanate which leads to higher chemical pressure in the former compound. Thus, in the first place it was of interest to compare the values of the entropy changes associated with the similar individual transformations in $(NH_4)_3SiF_7$ and $(NH_4)_3GeF_7$.

Fig. 6c demonstrates that the temperature behavior of the excess entropy in silicate is complicated similar to germanate [14] due to overlapping of $\Delta S_i(T)$ contributions associated with the individual transformations. In order to determine the values of ΔS_i, we analyzed the $\Delta C_p(T)$ dependence in the framework of the Landau thermodynamic theory which was successfully used earlier for $(NH_4)_3GeF_7$ [14]. One of the important consequences of the Landau theory is that the value $(\Delta C_p/T)^{-2}$ is a linear function of the temperature below a point of the second/first order transformations close to the tricritical point [20]:

$$\left(\frac{\Delta C_p}{T}\right)^{-2} = \frac{2B}{A_T^2} + \frac{12C}{A_T^3}(T_0 - T). \quad (3)$$

Here T_0 is a temperature of phase transition, A_T, B and C are the coefficients of the thermodynamic potential $\Delta\Phi(p,T,\eta) = A_T(T-T_0)\eta^2 + B\eta^4 + C\eta^6$, where η is order parameter.

In the case of $(NH_4)_3SiF_7$, analysis of $\Delta C_p(T)$ using Eq. (3) can be performed only for succession of transitions $P4/mbm \leftrightarrow Pbam \leftrightarrow P2_1/c11 \leftrightarrow P\bar{1}$ because all of these phases are connected with each other by the group-subgroup relationship, while the fourth transformation $P\bar{1} \leftrightarrow P12_1/c1$ is of the reconstructive type [15].

The linear temperature dependencies of $(\Delta C_p/T)^{-2}$ were found below T_1, T_2 and T_3 over different ranges of the temperature $T_1 - T \approx 6$ K, $T_2 - T \approx 1$ K, $T_3 - T \approx 7$ K and were characterized by different slope (Fig. 7). Due to the absence of information on the A_T coefficient associated with the elastic susceptibility, using Eq. (3) it was possible to determine only combination of the coefficients of the thermodynamic potential $\Delta\Phi(p, T, \eta)$. In accordance with Ref. [20], the combination of these parameters allows one to characterize the proximity of the second and first order phase transitions to the tricritical point T_k characterized by $(\Delta C_p/T)^{-2} = 0$.

$$N = \left(B^2/3A_T C T_0\right)^{1/2} = [(T_k - T_0)/T_0]^{1/2}. \quad (4)$$

Small values of the parameters N_{Ti} (Table 2) show that phase transitions $P4/mbm \leftrightarrow Pbam \leftrightarrow P2_1/c \leftrightarrow P\bar{1}$ in $(NH_4)_3SiF_7$ are rather close to the tricritical point. It is seen also that the Si → Ge substitution led only to small change in the N_{Ti} value for transformations at T_1 and T_2.

The contributions of $\Delta C_p(T)$ existed below T_1, T_2 and T_3 and described by Eq. (3) can be extrapolated into $P2_1/c11$, $P\bar{1}$ and $P12_1/c1$ phases, respectively (Fig. 8a). As a result, the anomalous behavior of $\Delta C_p(T)$ near the phase transition into the phase $P12_1/c1$ appears as shown in Fig. 8b. Then, it was possible to determine the entropy changes for each individual phase transition (Table 2).

Taking into account the overlapping of the anomalous heat capacity contributions and the uncertainty of determining the excess entropy when integrating the $(\Delta C_p/T)(T)$ function, the magnitudes of ΔS_1 and ΔS_2 in silicon and germanium compounds can be considered as rather close (Table 2).

Moreover, as it seen in Fig. 8a, a small smeared bump of ΔC_p exists at $T_1' \approx 240$ K in *Pbam* phase of $(NH_4)_3SiF_7$. It is impossible to imagine the

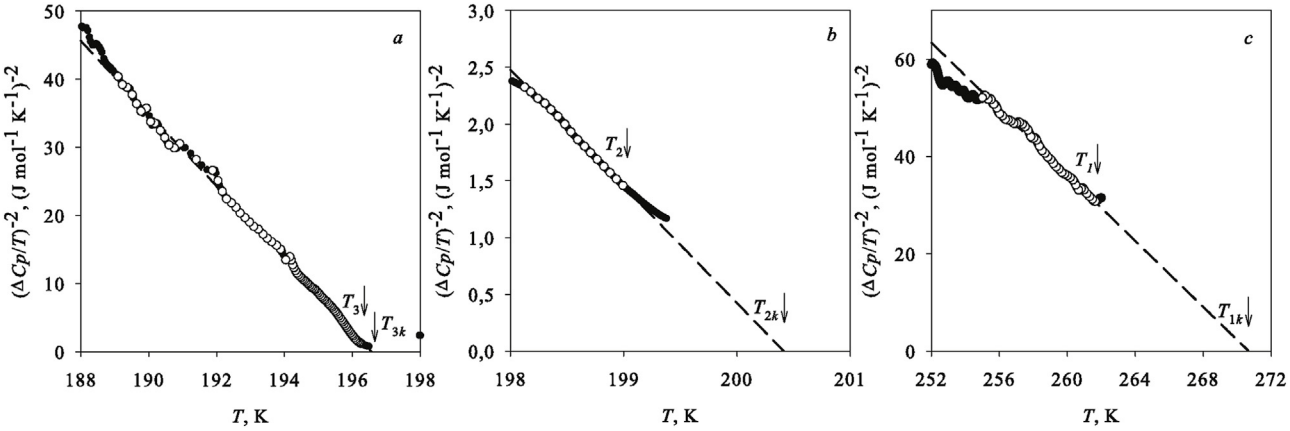

Fig. 7. Temperature dependence of the square of the inverse excess heat capacity in the vicinity of (a) T_1, (b) T_2 and (c) T_3.

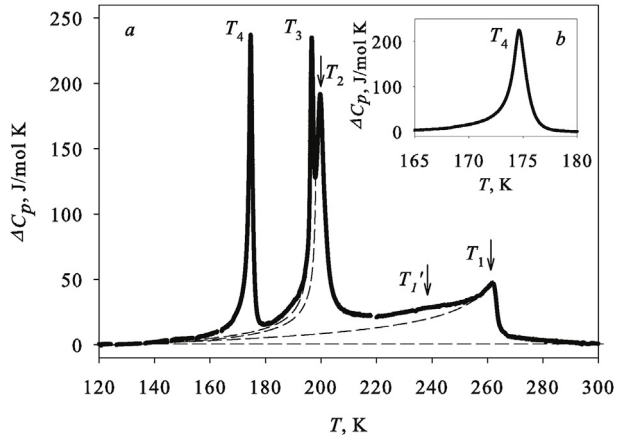

Fig. 8. (a) Temperature dependence of the total excess heat capacity. Dashed lines present the behavior of contributions into $\Delta C_p(T)$ in the intermediate (*Pbam*, $P2_1/c$ and $P\bar{1}$) and low temperature $P2_1/c$ phases. (b) Temperature dependence of excess heat capacity around T_4.

origin of this anomaly because any pronounced peculiarities in the behavior of other physical properties studied in this paper and in Ref. [13] were not observed between T_1 and T_2. Rough estimate of entropy change around T_1' gives the value about $\Delta S_1' = 0.5 \pm 0.2$ J/mol·K In such a case ΔS_1 in $(NH_4)_3SiF_7$ will be more close to the same for $(NH_4)_3GeF_7$.

Analysis of the X-ray data has shown that all NH_4 groups disordered in the initial phase $P4/mbm$ are fully ordered in the lowest-temperature phase $P12_1/c1$ due to emergence of N—H···F hydrogen bonds [13]. In accordance with the data presented in Table 2, phase transitions in silicate are characterized by rather strong difference in the entropy. Large values of entropy which could be associated with the order-disorder processes were found only for transformations at T_1 ($\Delta S_1 \approx R \ln 3$) and T_2 ($\Delta S_2 \approx R \ln 2$). On the other hand, mechanism of the phase transition $P2_1/c11 \leftrightarrow P\bar{1}$ can be considered as associated with insignificant displacements of the structural elements leading to very small entropy change $\Delta S_3 \approx 0.1R$. Thus, the total ordering of the structural units in silicon compound takes place in the monoclinic phase $P2_1/c11$.

Large difference between the changes of entropy and volume deformation at the reconstructive transformations in $(NH_4)_3SiF_7$ ($\Delta S_4 \approx 0.4R$; $\delta(\Delta V/V_0 \approx -0.4)$% and $(NH_4)_3GeF_7$ ($\Delta S_3 \approx 1.6R$; $\delta(\Delta V/V_0 \approx -1.0$% [14]) can be explained by less symmetry change at T_4 and as result by less displacements of atoms in the former compound ($P\bar{1} \leftrightarrow P12_1/c1$) [15] compared to $P2_1/c11 \leftrightarrow Pa\bar{3}$ found in germinate at T_3 [13].

The validity of the thermodynamic approach used to determine the anomalous heat capacities and entropies associated with the individual phase transitions was confirmed by comparison of the data obtained in three independent experiments: $\beta(T)$, $C_p(T)$ and $T(p)$. Using the data on $\Delta\beta_i$ and ΔC_{pi} in the framework of the Ehrenfest equation for the second order transformations $Pbam \leftrightarrow P2_1/c11$ and $P2_1/c11 \leftrightarrow P\bar{1}$, the values of relative baric coefficients were determined, $dT_2/dp = -43$ K/GPa and $dT_3/dp = -58$ K/GPa, which are in a good agreement with the results of direct measurements above (Table 2).

For the first order transition $P\bar{1} \leftrightarrow P12_1/c1$, the value $dT_4/dp = -54$ K/GPa calculated using the Clausius-Clapeyron equation also agrees well with the baric coefficient determined in DTA experiments with pressure (Table 2).

These facts unambiguously show the reliability of the information about thermal properties obtained by the three independent experimental methods.

Above we showed that direct measurement of dT_1/dp was impossible because of a quick smearing and disappearance of the heat capacity anomaly at T_1 under pressure. Calculation of this baric coefficient using the Ehrenfest equation shows the magnitude, $dT_1/dp \approx 15$ K/GPa, which rather close to the same parameter found for $(NH_4)_3GeF_7$ ($dT_1/dp = 10$ K/GPa) [14]. In accordance with the calculated value, the boundary between phases $P4/mbm$ and *Pmba* is shown by the dashed line in Fig. 5. Thus, the increase in pressure leads to the expansion of the temperature range of the *Pbam* phase existence just as it was observed for germanate [14].

4. Conclusions

In the present paper, detailed studies of heat capacity, thermal expansion, dielectric properties and sensitivity to hydrostatic pressure at the rich sequence of phase transitions $P4/mbm \leftrightarrow Pbam \leftrightarrow P2_1/c11 \leftrightarrow P\bar{1} \leftrightarrow P12_1/c1$ in the fluoride double salt $(NH_4)_3SiF_7$ have been performed.

The properties investigated have shown anomalous behavior at all structural transformations which were found to be of nonferroelectric origin in accordance with the temperature dependencies of permittivity and dielectric losses.

Reconstructive phase transition accompanied by an increase in symmetry $P\bar{1} \leftrightarrow P12_1/c1$ upon cooling and strong jump in deformation and enthalpy corresponds to a pronounced transition of the first order.

The total change in the entropy associated with successive transformations in $(NH_4)_3SiF_7$ is characterized by the minimal value $\sum \Delta S_i = 19$ J/mol K compared to the other double fluoride salts $(NH_4)_3MeF_7$ (J/mol K): 32 (Me = Ti), 32.5 (Sn), 25.5 (Ge) [10,12,14]. Such a large difference is most likely a result of the absence of structural distortions in silicate associated with transitions into cubic phases $Pm\bar{3}m$ and $Pa\bar{3}$.

The behavior of the excess heat capacity below transition points T_1, T_2 and T_3 follows to the Landau thermodynamic theory and allows one to determine the entropies associated with each individual structural transformation. The succession of the symmetry changes $P4/mbm \leftrightarrow Pbam \leftrightarrow P2_1/c$ realized in related $(NH_4)_3SiF_7$ and $(NH_4)_3GeF_7$ crystals is associated with close entropy values: Si – $\Delta S_1 + \Delta S_2 \approx 14.3$ J/mol·K; Ge – $\Delta S_1 + \Delta S_2 \approx 12.0$ J/mol K [14].

The entropic parameters also show that order-disorder processes occur during transformations at T_1 ($\Delta S_1 \approx R \ln 3$) and T_2 ($\Delta S_2 \approx R \ln 2$). Very small entropy change at T_3 ($\Delta S_3 \approx 0.1R$) proves the displacive mechanism of the corresponding phase transition. However, transformation at T_4 is characterized by rather large entropy $\Delta S_4 \approx 0.4R$ which can be associated with the final complete ordering of ammonium groups [15]. Thus, these experimental facts suggest that the complete ordering of the structural elements takes place in the monoclinic phase $P12_1/c1$ of $(NH_4)_3SiF_7$.

Good agreement between measured and calculated baric coefficients proves the reliability of the results obtained. The $T-p$ phase diagram demonstrates that the temperature range of the orthorhombic phase *Pbam* expands with increasing pressure similar to related fluoride $(NH_4)_3GeF_7$ [14]. The intervals of existence of two monoclinic and triclinic phases do not depend on the pressure.

Acknowledgements

The authors thank Dr. M.S. Molokeev for X-ray characterization of the samples.

References

[1] I. Flerov, M. Gorev, K. Aleksandrov, A. Tressaud, J. Grannec, M. Couzi, Phase transitions in elpasolites (ordered perovskites), Mater. Sci. Eng. R Rep. 24 (3) (1998) 81–151. https://doi.org/10.1016/S0927-796X(98)00015-1.

[2] M.V. Gorev, I.N. Flerov, A. Tressaud, Thermodynamic properties and p-t phase diagrams of $(NH_4)3M^{3+}F6$ cryolites (m^{3+}: Ga, sc), J. Phys. Condens. Matter 11 (39) (1999) 7493–7500. https://doi.org/10.1088/0953-8984/11/39/306.

[3] T. Nakajima, B. Zemva, A. Tressaud, Advanced Inorganic Fluorides: Synthesis, Characterization and Applications, Elsevier Science.

[4] I. Flerov, M. Gorev, J. Grannec, A. Tressaud, Role of metal fluoride octahedra in the mechanism of phase transitions in A_2BMF_6elpasolites, J. Fluorine Chem. 116 (1) (2002) 9–14. https://doi.org/10.1016/S0022-1139(02)00068-4.

[5] A. Tressaud (Ed.), Functionalized Inorganic Fluorides: Synthesis, Characterization and Properties of Nanostructured Solids, Wiley-Blackwellhttps://doi.org/10.1002/9780470660768.

[6] M. Leblanc, V. Maisonneuve, A. Tressaud, Crystal chemistry and selected physical properties of inorganic fluorides and oxide-fluorides, Chem. Rev. 115 (2) (2015) 1191–1254. https://doi.org/10.1021/cr500173c.

[7] J. Ravez, Ferroelectricity in solid state chemistry, C.R. Acad. Sci. - Ser. IIC - Chem. 3 (4) (2000) 267–283. https://doi.org/10.1016/S1387-1609(00)00127-4.

[8] M. Molokeev, S.V. Misjul, I.N. Flerov, N.M. Laptash, Reconstructive phase transition in $(NH_4)_3TiF_7$ accompanied by the ordering of TiF_6 octahedra, Acta Crystallogr. Sect. B Struct. Sci. 70 (6) (2014) 924–931. https://doi.org/10.1107/S2052520614021192.

[9] S. Mel'nikova, E. Pogoreltsev, I. Flerov, N. Laptash, Unusual sequence of phase transitions in $(NH_4)_3$ TiF_7 detected by optic and calorimetric studies, J. Fluorine Chem. 165 (2014) 14–19. https://doi.org/10.1016/j.jfluchem.2014.05.016.

[10] E. Pogoreltsev, I. Flerov, A. Kartashev, E. Bogdanov, N. Laptash, Heat capacity, entropy, dielectric properties and tp phase diagram of $(NH_4)_3TiF_7$, J. Fluorine Chem. 168 (2014) 247–250. https://doi.org/10.1016/j.jfluchem.2014.10.016.

[11] I. Flerov, M. Molokeev, N. Laptash, A. Udovenko, E. Pogoreltsev, S. Mel'nikova, S. Misyul, Structural transformation between two cubic phases of (nh4)3snf7, J. Fluorine Chem. 178 (2015) 86–92. https://doi.org/10.1016/j.jfluchem.2015.06.024.

[12] A. Kartashev, M. Gorev, E. Bogdanov, I. Flerov, N. Laptash, Thermal properties and phase transition in the fluoride, $(NH_4)_3SnF_7$, J. Solid State Chem. 237 (2016) 269–273. https://doi.org/10.1016/j.jssc.2016.02.027.

[13] S.V. Mel'nikova, M.S. Molokeev, N.M. Laptash, S.V. Misyul, A non-typical sequence of phase transitions in $(NH_4)_3GeF_7$: optical and structural characterization, Dalton Trans. 45 (2016) 5321–5327. https://doi.org/10.1039/C5DT04907E.

[14] E. Bogdanov, A. Kartashev, E. Pogoreltsev, M. Gorev, N. Laptash, I. Flerov, Anomalous behaviour of thermodynamic properties at successive phase transitions in $(NH_4)_3GeF_7$, J. Solid State Chem. 256 (2017) 162–167. https://doi.org/10.1016/j.jssc.2017.09.010.

[15] S.V. Mel'nikova, M.S. Molokeev, N.M. Laptash, E.I. Pogoreltsev, S.V. Misyul, I.N. Flerov, Sequence of phase transitions in $(NH_4)_3SiF_7$, Dalton Trans. 46 (2017) 2609–2617. https://doi.org/10.1039/C6DT04874A.

[16] M. Gorev, E. Bogdanov, I. Flerov, T-p phase diagrams and the barocaloric effect in materials with successive phase transitions, J. Phys. D Appl. Phys. 50 (38) (2017) 384002. https://doi.org/10.1088/1361-6463/aa8025.

[17] M. Gorev, E. Bogdanov, I. Flerov, Conventional and inverse barocaloric effects around triple points in ferroelastics $(nh_4)_3nbof_6$ and $(nh_4)_3tiof_5$, Scripta Mater. 139 (2017) 53–57. https://doi.org/10.1016/j.scriptamat.2017.06.022.

[18] M. Marignac, Rech, formes crist. composition chim. divers sels, Ann. Min. 15 (1859) 221–290.

[19] A.V. Kartashev, I.N. Flerov, N.V. Volkov, K.A. Sablina, Adiabatic calorimetric study of the intense magnetocaloric effect and the heat capacity of $(La_{0.4}Eu_{0.6})_{0.7}Pb_{0.3}MnO_3$, Phys. Solid State 50 (2008) 2115–2120. https://doi.org/10.1134/S1063783408110188.

[20] K.S. Aleksandrov, I.N. Flerov, The applications of the thermodynamic theory to structural phase transitions close to the tricritical point, Fiz. Tverd. Tela 21 (1979) 327–336.